CFD Simulation of UV Disinfection Reactor for Applesauce with a Low UV Absorption Coefficient

Seyed Hassan Hashemabadi[*1], Farkhondeh Ghaderzadeh[1] and FariborzTaghipour[2]
[1]Computational Fluid Dynamics (CFD) Research Laboratory, School of Chemical Engineering, Iran University of Science and Technology (IUST), Tehran, Iran
[2]Department of Chemical and Biological Engineering, University of British Columbia, Vancouver, BC Canada
(Received 16 December 2013, Accepted 8 September 2014)

Abstract

In this study, a Computational Fluid Dynamics (CFD) model was developed to evaluate ultraviolet disinfection applesauce reactor. To simulate UV reactors, three sets of equations, including hydrodynamics, radiation and species mass conservation were solved simultaneously. The Realizable k-ε turbulence model and the discrete ordinate method were used to find the UV radiation profile through the reactor. Using the Chick-Watson kinetic model and the Eulerian framework, inactivation of applesauce microorganisms was simulated in the UV reactor. Simulation results for water disinfection in the UV reactor were evaluated by the reported experimental data. Simulation was extended for non-Newtonian fluid such as applesauce. Results show that the UV reactor is less effective in eliminating microorganisms from applesauce than from water because applesauce has a higher UV absorption rate. In order to achieve higher disinfection of the UV reactor for non-Newtonian fluids with high absorption, this study examined different parameters and makes suggestions for appropriate reactor design. Different designs for disinfection reactor were studied, due to higher UV absorption coefficient of applesauce, CFD simulations show that the inactivation of microorganisms in applesauce is less than water, consequently thin film or small radius reactors are appropriate design.

Keywords: Computational fluid dynamics (CFD), Disinfection, Ultraviolet (UV) reactor, Non-Newtonian fluid, Reactor engineering

Introduction

Liquid foods must be disinfected prior to sale and consumption in order to eliminate microbial growth. Currently, thermal pasteurization is the most widely available technique used to disinfect liquid food, but it is not without disadvantages. Thermal pasteurization is expensive, also impacts the flavor of the food, and the heat used in the process destroys sensitive nutrients. An alternative disinfectant method is thus useful to the liquid foods industry [1]. As non-chemical and non-thermal disinfection method, ultraviolet (UV) light, has recently achieved increased acceptance in the liquid food industry. UV radiation removes harmful microorganisms such as bacteria, viruses and yeasts from liquid food, and it is easy to maintain and consumes less energy than thermal pasteurization. UV radiation is also an environmentally compatible technology because it achieves high levels of disinfection without chemical treatment.

UV radiation has previously been used to disinfect liquid foods such as apple juice, apple cider [2-4], orange juice, and melon, carrot, guava and pineapple juice [5 and 6]. Koutchma & Parisi [3] studied the flow pattern of apple juice and apple cider in UV reactors. They concluded that turbidity and amount of UV that fluid absorbs (the absorbance of a sample is the negative logarithm of the UV transmittance) is an important factor in disinfectant process. Microbial inactivation tests using a cocktail of strains are also important to consider in conjunction with UV disinfection [7]. Non-thermal UV processing has the appropriate potential to develop the safety and properties of liquid egg [8].

A benefit of UV reactor simulation is that the virtual prototypes reduce costs and allow for evaluation of design alternatives. As a result of recent growth in numerical simulation, computational fluid dynamics(CFD) is becoming a powerful,

* Corresponding author: Tel: +98-21-77240376 Fax: +98-21-77240495 Email: hashemabadi@iust.ac.ir

straightforward and economical engineering method to simulate and optimize reactor designs. CFD requires simultaneously solving hydrodynamic, radiation and kinetic equations. The continuity and momentum equations in the turbulence model are solved together to obtain the velocity profile and flow field. Then, the radiation models are applied in order to calculate the radiation distribution. Using the kinetic models, velocity values and radiation rate, the reactor performance is calculated to determine the inactivation of microorganisms.

The majority of prior CFD simulations of UV reactors have applied to Newtonian fluids with low absorption factors. Most published CFD simulations involved water treatment [9-14] while simulations involving liquid food are rare. Unluturk et al. (2004) simulated an apple juice and apple cider UV reactor [1]. They assumed, however, that apple juice and apple cider have Newtonian behavior, and therefore they used Dispersed Phase Method (DPM), Linear Source Infinite (LSI), and Multiple Point Source Summation (MPSS) radiation models to predict the UV reactor performance. To our knowledge, there is no published CFD simulation of UV reactor for processing of non-Newtonian fluids. Almost all liquid foods follow non-Newtonian models and some of them have high UV absorption coefficients. The present work investigates and takes into account the CFD simulation of UV disinfection reactor for these fluids.

2. Governing equations

2.1. Flow model

The mass and momentum conservation equations must be solved together for calculation of flow field and velocity profile. Reynolds Averaged Navier Stokes (RANS) equations have been solved in steady state condition without source term [1 and 14]:

$$\nabla \cdot (\rho u) = 0 \tag{1}$$

$$\nabla \cdot (\rho u u) = -\nabla p - \nabla \cdot (\tau + \tau^t) + \rho g \tag{2}$$

The flow inside the reactor is complex as it involves the generation of swirl produced by the positioning of the outlet at a 90-degree angle to the original flow direction. The turbulence stress tensor τt (in Eq. 2) has been calculated by Realizable k-ε turbulence model. In this technique in addition the continuity and momentum equations, two other equations include turbulence kinetic energy (k) and rate of energy dissipation (ε) must be solved. The turbulent viscosity νt and turbulence stress tensor can be obtained by following equations, respectively:

$$\nu_t = \frac{C_\mu k^2}{\varepsilon} \tag{3}$$

$$\tau^t = \nu_t \left(\frac{\partial u_i}{\partial x_j} + \frac{\partial u_j}{\partial x_i} \right) - \frac{2}{3} k \delta_{ij} \tag{4}$$

2.2. Radiation model

The fluence rate can be obtained by solving radiation models as a function of the distance from the lamp and the UV transmittance. In general, radiation models can be divided to four categories. In the first category lamp is divided to n equal points along the axis of the lamp and the fluence rate is calculated in each point. The total fluence rate is obtained with summation of fluence rate in each point. The most important model in this group is Multiple Point Source Summation (MPSS) model. In the second category, lamp is divided to n equal segment along the axis of the lamp and fluence rate is calculated in each segment. Similar to previous group, the total fluence rate is calculated with the summation of fluence rate in each segment. One of the most important models in this category is Multiple Segment Source Summation(MSSS) [14]. In the third class, lamp is considered a line source of radiation like as LSI (Linear Source Infinite) [14]. In other word, these types are integral of two previous models. Forth category is Discrete

Ordinate (DO) method. In this study three radiation models including MPSS, LSI and DO are investigated. In MPSS model without considering refraction and reflection, the fluence rate is obtained by [14]:

$$I(r,z)=\sum_{i=1}^{n}\frac{\phi/n}{4\pi l_i^2}\exp\left(-\sigma_w\left(r-r\right)_L\frac{l_i}{r}\right) \quad (5)$$

Where I is fluence rate that is a function of absorption coefficient (σw) and distance (r). Absorption coefficient can be obtained from the transmittance (Tr) and can be calculated as:

$$\sigma_w=\ln(Tr) \quad (6)$$

The continuous version of the MPSS model is the LSI model [15]. The LSI model is an efficient method that does not need complicated numerical solution and ignores refraction and reflection of radiation. The fluence rate is obtained by [14]:

$$I(r)=\frac{\phi}{2\pi r L_2}\exp\left(\sigma_w(r-r_L)\right) \quad (7)$$

In DO model, the radiation equation is solved by considering of absorption and scattering terms.

The equation of this model can be expressed as:

$$\nabla.(I(\bar{r},\bar{s})\bar{s})+(\sigma_w+k_s)I(r,\Omega)-\sigma_w n^2\frac{\sigma T^4}{\pi}-\frac{k_s}{4\pi}\int_{4\pi}I(r,\Omega)\varphi(\Omega'\rightarrow\Omega)d\Omega'=0 \quad (8)$$

According to Eq. (8), the first term is the gradient of intensity along diffusion direction. Other terms are losing due to absorption, out scattering, emission of black body, and receiving due to in scattering [16] respectively. Stamnes et al. [17] used DO model with reflection which takes place at the interface of the layers. Liou et al. [18] developed the DO model for the simulation of radiation transfer in a multi-layer medium [17]. Applesauce, the fluid in this article, has particles. The DO model is sufficient model for this, because DO model considers emission and scattering particles.

2.3. Disinfection kinetics model

In this study, MS2 (E. coli bacteriophage ATCC 15597-B1) was considered as the model microorganism for inactivation. For MS2, the inactivation rate by UV radiation can be approximated using first order Chick-Watson kinetics as:

$$R=-K\,I\,C \quad (9)$$

Where K is the inactivation rate constant that it has been reported as 0.01 m2/J[14].

2.4. Integrated reactor performance model

In order to simulate the UV reactor, it is important to determine the path microorganisms will follow in the reactor. Two frameworks, Eulerian and the Lagrangian, are available to detect the trajectory of microorganisms in the reactor. In this paper, Eulerian approach was used, which assumes all microorganism species are the continuous phase components. Additionally, inactivation volumetric rates in the disinfection kinetic models were implemented as source terms in the mass conservation equations. The concentration of species in steady state condition can be determined by the following equation:

$$\nabla\cdot(u\,C)=-\nabla\cdot\left(D\nabla C\right)+R \quad (10)$$

Where D is the diffusion coefficient. Solving the species equation facilitates calculating the concentration of microorganisms; and the inactivation rate can be obtained using the logarithm: initial concentration divided by local concentration (Log (C0/C)) [14].

3. Geometry of the reactor, boundary conditions and CFD simulation

The UV reactor used in this simulation follows the design proposed by Sozzi & Taghipour [14] (Figure 1). Thereactor's diameter is 89 mm, its length is 889 mm and the diameter of the UV lamp in the center of the reactor is 20 mm. The inlet and outlet pipes are 850 mm long and 19.1 mm in diameter. The inlet port is centered in front of the UV reactor and the outlet port is placed 25.4 mm far from the end of the reactor. To create a fully developed flow, the inlet port is designed approximately 45 times the diameter of the inlet. The UV lamp is held in the center of the reactor.

Table 1: Detail dimension of UV reactor

Dimension	Diameter (mm)	Length (mm)
Reactor body	89	889
Lamp	20	800
Inlet and outlet pipe	19.1	850

Table 1 shows a detail of the dimensions of the reactor. Structured and unstructured mesh reactors were used in these simulations. Structured mesh reactors were divided into several domains and each sub-domain mesh was constructed separately.

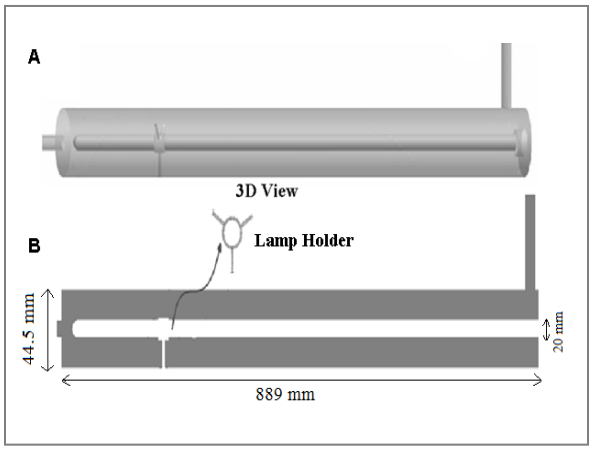

Figure 1: Geometry of UV reactor A) 3D View B) Longitudinal cross section

Inlet and outlet pipe grids were 5700 structured mesh. All sub-domains mesh was structured, except near the holder where it was meshed with tetrahedral unstructured mesh. The governing equations are solved by finite volume approach [19 and 20]. Internal structures were implemented as 3D volumes. Furthermore, no-slip boundary condition were set at the reactor and lamp walls; and mass flow rate and outflow boundary conditions were chosen for inlet and outlet boundary conditions. The value of the turbulence intensity was adjusted 10%. The velocity coupling SIMPLE method was applied to account for pressure, and the first order upwind discretization advection scheme was implemented for the segregated steady-state solver.

Inorder to evaluate the reactor performance model, an initial simulation was performed using water disinfection with a UV reactor that had a volumetric inlet rate of 0.65 kg/s and 35.66 m-1 of absorption coefficient in 298K and wavelength of 254 nm. After this step, the fluid was changed to the non-Newtonian fluid applesauce. In 299K, applesauce has 0.45 of power law index and 7.32 Pa.sn consistency coefficients in the range of 0.78-1260 s-1 shear rate. The UV absorption coefficient for applesauce is 2100 m-1 in wavelength of 254 nm and density is 1070 kg/m3.

Table 2: Characteristics of water and applesauce [21] at 299 K

Fluid	Density (kg/m^3)	n	K (pas^n)	Shear rate (s^{-1})	Absorption coefficient (m^{-1})
Water	998	1	-	-	35.66
Apple sauce	1070	0.45	7.32	0.78-1260	2100

The respective physical properties of water and applesauce are given in Table 2 [21].

4. Result and discussion

4.1. Mesh independency and validation of model

In this study structured and unstructured grid was used for simulating the flow through the reactor. Figure 2 shows four different meshes that have been

implemented in simulation. Intel® Core™ i7-965 Processor (8M Cache, 3.20 GHz) with 6 GB RAM has been used for simulations. Table 3 illustrates average relative error respect to Sozzi &Taghipour [22] work for velocity profile at 64 cm from reactor entrance. As it can be seen from this table the difference between the results of the grids more than 300000 is less than 4% but the computational time increases more than 50 percent, consequently the 300000 structured meshes have been applied.

Table 3: Average relative error respect to reference [22] for velocityprofile at 64 cm far from reactor entrance

	Mesh Size	Mesh Type	Time* (hr)	A.R.E** (%)
A	50000	Structured	18	12
B	300000	Structured	120	4.8
C	1400000	Structured	190	4.6
D	1200000	Unstructured	240	10

*Computation Time,**Average Relative Error

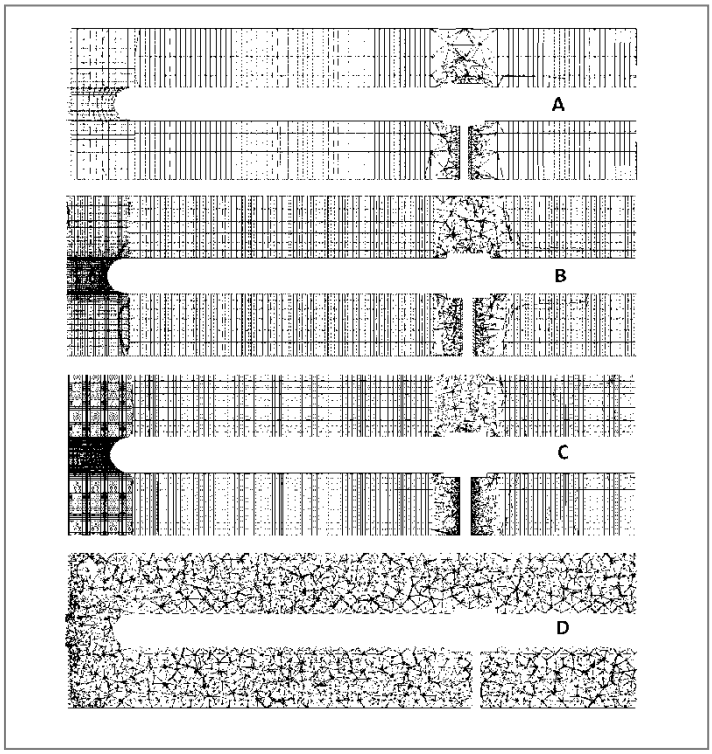

Figure2: Four different meshes
A) 50000 Structured, B) 300000 Structured, C) 1400000 Structured, D) 1200000 Unstructured

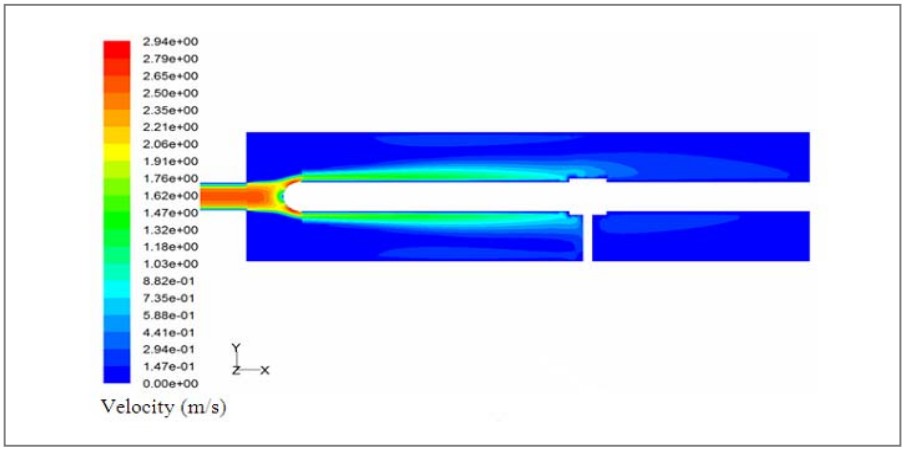

Figure 3: Contours of velocity in water UV reactor (0.65 kg/s mass flow inlet)

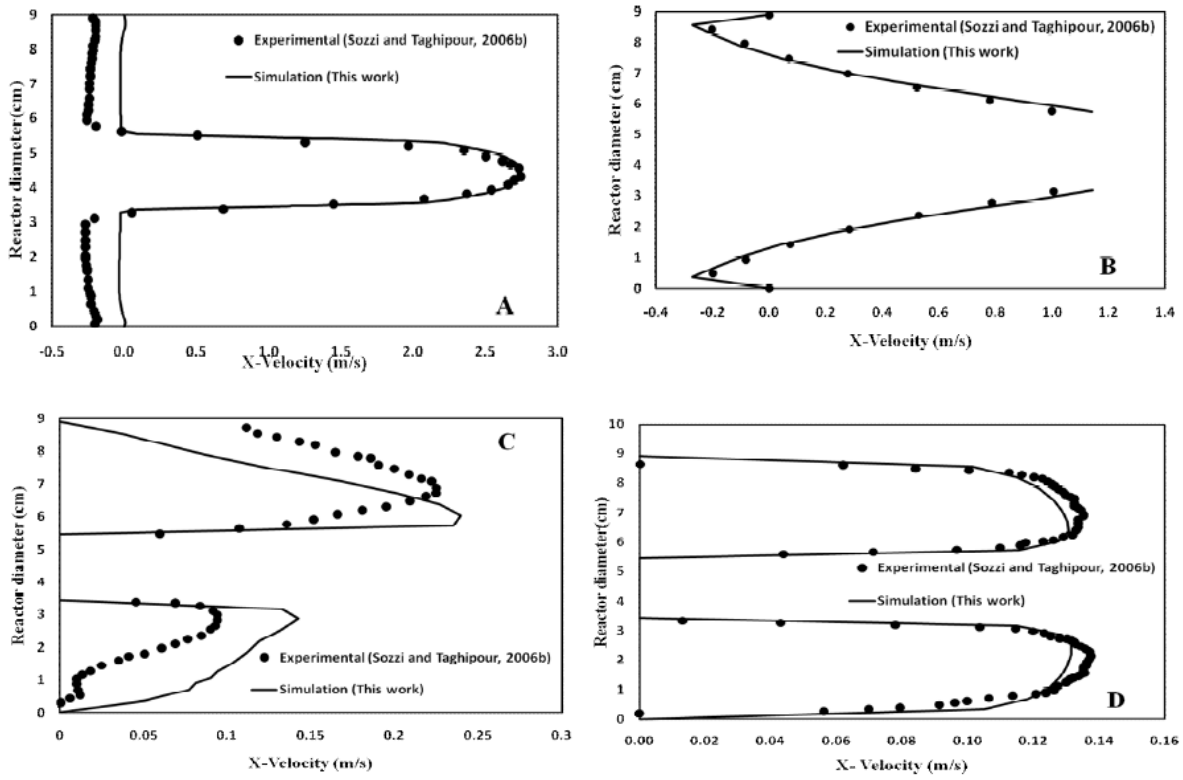

Figure 4: Comparison of velocity profile between the simulation and experimental results [22] at A) 1cm, B) 15 cm, C) 23 cm, D) 64 cm from the reactor inlet

The initial validation case involved disinfecting water using a UV reactor. In this step, the flow field and velocity profile were obtained by solving RANS equations (Eqs.1 and 2) with proper boundary conditions. It should be noted that in these simulations power law, non-Newtonian fluid model (power law and consistency indices and water viscosity are equal to 1) has been implemented. Figure 3 shows velocity contours in the water UV disinfection reactor. According to Figure 3, fluid co-axially enters at the reactor inlet then collides with the lamp. The flow then separates and keeps its symmetric form. Figure 4 compares the velocity profile with the experimental results [22] at 1, 15, 23 and 64 cm from the inlet of the reactor with a 0.65 kg/s mass flow inlet. Figure 4 demonstrates that the water simulation results closely reflected the Particle Image Velocimetry (PIV) data.

According to Figure 4C, the results showed more deviation from the experimental data at 23 cm from the inlet of the reactor. The deviation can be explained by the use of unstructured mesh in the location of the lamp holder in the UV reactor.

Figure 5 compares the contour of fluence rate from the DO radiation model with the MPSS and LSI models prediction investigated by Sozzi &Taghipour [14]. The power of the UV lamp for the three radiation models was set at 35 Watts. The maximum radiation is located on the surface of the lamp, thus the fluence rate decreased radically from the lamp surface to the reactor body. The LSI model cannot predict clear radiation in the arc of the lamp (see Figure 5A; there is no radiation distribution at thearc), but the MPSS and DO models

can calculate the arc radiation. Figure 6 shows the radial distribution of the fluence rate at 50 cm from the reactor entrance for the MPSS, LSI and DO models. According to these results,the fluence rate declines further away from the lamp.

The fluence rates clearly show the differences among the three different model predictions. The fluence rate for the MPSS model from the reactor walls to the lamp ranges from 40 to 900 W/m2, the range for the LSI model is from 50 to 600 W/m^2 and for the DO model it is 50 to 700 W/m^2. It is possible to conclude that the MPSS model predicted the maximum fluence rate and the result of the DO model is intermediate of the other two. Also, the results show that at various points away from the UV lamp, the three models predict almost the same radiation intensity. The three models predict acceptable amounts of radiation at distances of 3 cm and more from the lamp. These results coincide with the UV fluence rate measurements on the basis of actinometry [14 and 23].

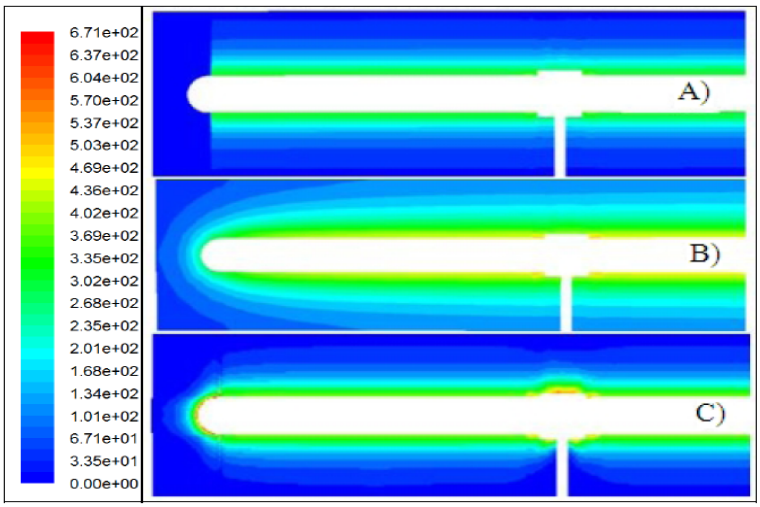

Figure 5: The radiation distribution in UV reactor
A) LSI model [14] B) MPSS model [14] C) DO model (This work)

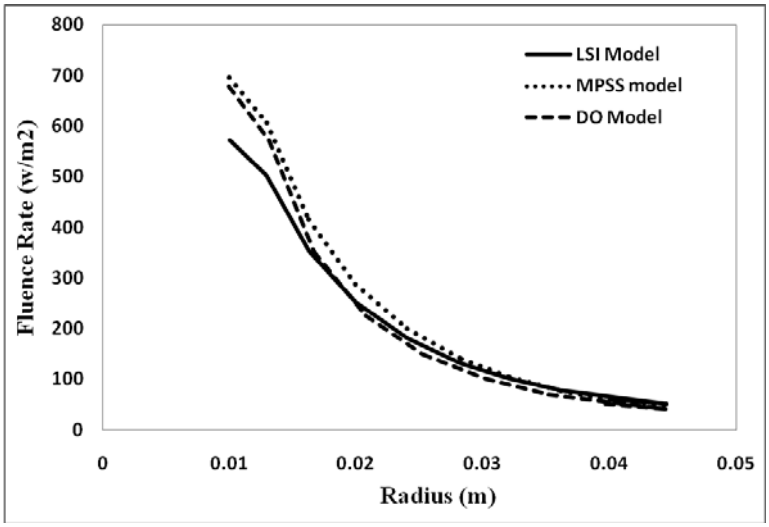

Figure 6: Fluence rate versus radius for MPSS, LSI and DO models

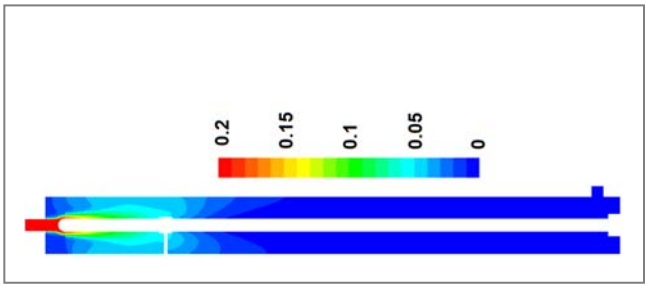

Figure 7: Contours of mass fraction of living microorganism concentration in water

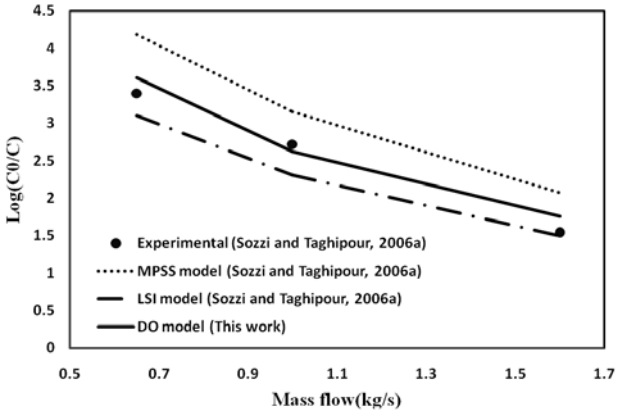

Figure 8: Living microorganism inactivation rate in different mass flow rate with three different radiation models

4.2. Performance of the water UV disinfection reactor

The mass fraction of microorganisms was obtained by solving the hydrodynamic equations, radiation models, the Chick-Watson kinetic model and the Eulerian approach in species mass conservation. For simulation of LSI, MPSS models and Chick-Watson model code was written. Figure 7 indicates the mass fraction distribution of living microorganisms in the UV reactor. The results show that the mass fraction of living microorganism is high at the reactor entrance, and it decreases along the reactor. Figure 8 presents the inactivity of living microorganisms as obtained in different inlet mass flow rates using the three different radiation models. Increasing the inlet flow rate caused water to remain in the reactor for a shorter period of time which results in lower inactivation rates. This relative error is reported in Table 4 for different inlet mass flow rates.

4.3. Applesauce UV disinfection reactor

Simulation results for non-Newtonian fluids were checked using the analytical solution depicted in Figure 9.The analytically dimensionless velocity profile for a power law fluid (n=0.45 and K=7.32 Pa.sn) in laminar fully developed flow ($Q=6.28\times10^{-4}$ m3/s) through the annulus (between the UV lamp and reactor body) [24] has a same trend with the simulation results, and deviation is due to turbulence regime in simulation case. The bulk velocity (U) can be derived directly from the bulk volumetric flow rate Q (i.e. U= Q/Annulus flow area). Figure 9 also shows velocity difference between Newtonian and non-Newtonian fluid. It can be seen that the non-Newtonian velocity is completely different, the maximum velocity for Newtonian fluid is higher than power law fluid and the velocity for applesauce is higher in the vicinity of the walls.

Table 4: Relative error (%) for inactivation of living microorganism in comparison with experimental data [14]

Inlet mass flow rate (kg/s)	MPSS [14]	LSI [14]	DO (This work)
00.65	23	9	6
1	15	15	4
10.6	34	2.5	14

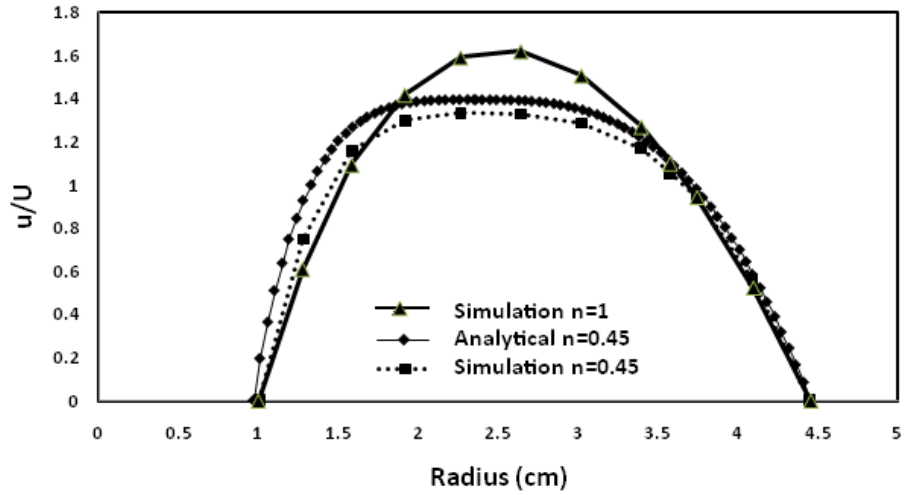

Figure9: Comparison of Newtonian, non-Newtonian and analytical solution velocity profile at 60 cm UV reactor entrance in Q=6.28×10^{-4}m3/s

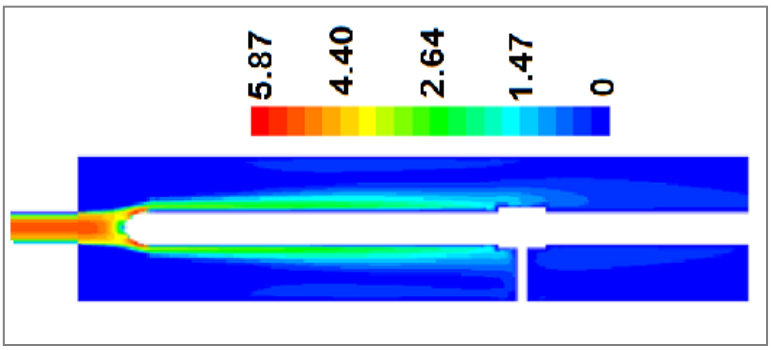

Figure 10: The velocity contours (m/s) for applesauce in 0.65 kg/s mass flow rate

Figure 10 illustrates that the velocity contours for applesauce are similar to those of water (Refer to Figure 3). Fluid enters the reactor via the entrance pipe and is separated after striking the lamp, but it keeps its symmetric form. The velocity profile is developed until the fluid reaches the lamp holder, at which time the fully developed region is obtained and the velocity profile remains unchanged. Due to lower apparent viscosity of applesauce, in a same condition the maximum velocity of flow through the reactor is approximately two times more than the water, consequently the residence time of pseudoplastic fluid (n=0.45) in reactor reduces considerably. In applesauce there are particles and high turbidity, since this

effect is usually appear as UV Transmittance, whereas it is very difficult to include the role of suspended particles with their possiblereflection or refraction properties, DO method is good model for this condition.

Based on the water UV reactor results, it is possible to conclude that in low mass inlet flow designs the DO is the proper radiation model. Therefore, the UV reactor with a low mass flow rate has been applied for applesauce. Figure 11 compares the fluence rate profile at 50 cm from the reactor entrance for water and applesauce. The fluence rate for applesauce is considerably lessthan for water because the UV absorption coefficient of applesauce is almost 60 times higher than water (see Table 2). In short, applesauce absorbs more UV radiation than water.

4.4. Performance of applesauce UV reactor

Figure 12 shows the distribution of living microorganisms in applesauce. Comparing disinfection results for applesauce (Figure 12) and water (Figure 7), it is apparent that UV disinfection is noticeably more effective on water than applesauce, and moreoverthe outlet mass fraction of microorganisms in applesauce is higher than water. The inactivation rate for applesauce is 0.078 for a 0.65 inlet mass flow rate; the same value for water is 3.61 (approximately 46 times lesser).Thus, the question becomes: what is the proper design for an applesauce reactor with very low UV absorption? To answer this question, we evaluated different designs that could increase applesauce reactor performance.

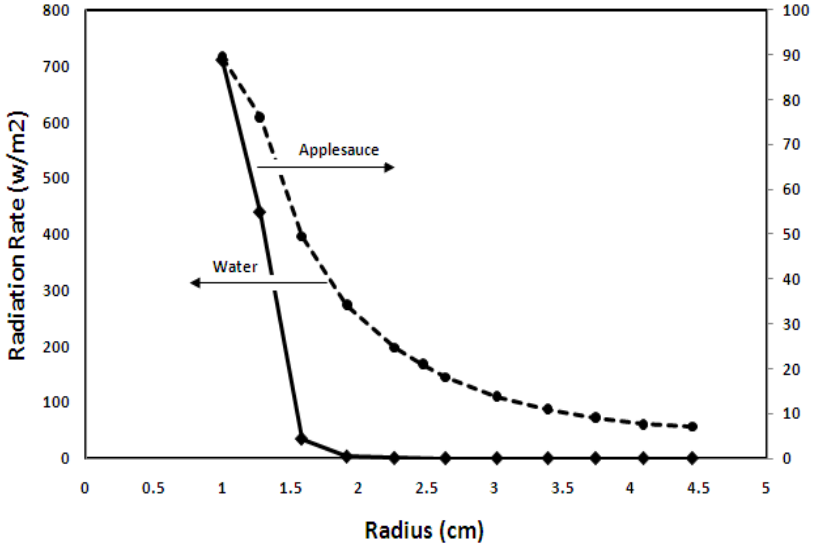

Figure 11: Fluence rate profile at 50 cm from reactor entrance for applesauce in with 0.65 kg/s mass flow rate

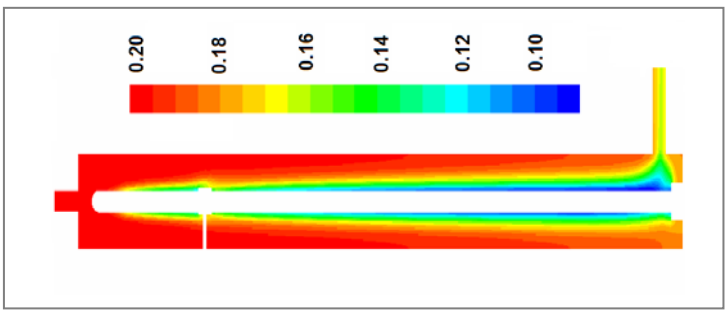

Figure12: Contours of mass fraction living microorganism for applesauce at 0.65 kg/s massFlow rate

This test also examined the effect of inlet mass flow rate on reactor performance. By decreasing the inlet mass flow rate from 0.1 kg/s to 0.01 kg/s, the inactivation rate per volume of the reactor can be enhanced from 85.46 m-3 to 683.89 m-3.Thus, it is apparent that the inactivation is high, but operating the reactor at low flow rate is not economical.

4.5. Influence of design on reactor performance

This section discusses the influence of different geometries on the test in terms of the inactivation rate of microorganisms. Geometry is very important for non-Newtonian UV reactors. According to the results (Figure 11), UV intensity reduces significantly more far from 1 cm of the lamp's surface so the geometry has to have less of 1cm radius.

Six reactor designs were simulated in different conditions and geometries. Five dimensions (reactors # 2 to # 6) were similar to the design proposed by Sozzi &Taghipour [14 and 22], but the radius or length of the reactors was different. Table 5 shows details of geometries for designs #2 to # 6. In reactor # 1, four lamps with the combined equivalent of one lamp's power (Figure 13) were used, and the simulation was done for 0.65 kg/s of mass flow rate. The mass fraction of live microorganisms is demonstrated in Figure 14. The results for the reactor #1 design clearly show that the mass fraction profile changed and the live microorganism concentration decreased.

Simulations were also completed for designs #2 and #3 with different radiuses (Table 5) at 0.65 kg/s mass flow rate. Table 6 shows that by decreasing the radius of reactor #3, the inactivation rate per volume increased significantly. Simulations were also performed in a constant feed mass flow rate (0.65 kg/s) for three other designs (#4 to #6), which are almost twice as long as the designs #2 and #3, though they have different radiuses (Table 5). The results show that by increasing the length of the reactor and the lamp, the inactivation rate per volume increases because the time the fluid is in contact with the UV light increases (Table 6). Two reactors, #5 and #6 (Table 5), were simulated with 0.1 kg/smass flow rate. As shown in Table 6, reactor # 6 provided superior inactivation per volume.

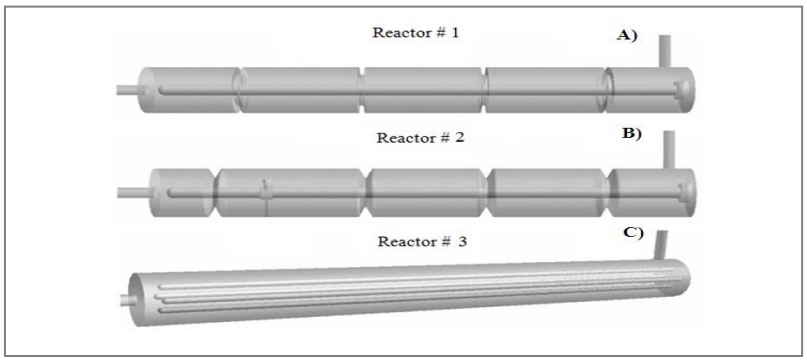

Figure 13: Investigation of different geometries A) reactor #1 cylindrical baffle B) reactor #2 Triangular baffle C) reactor #3Four lamps with summation of one lamp power

Table 5: Detail of geometries for designs #2 to #6

Design	Diameter (mm)	Length (mm)
Reactor # 2	49	889
Reactor # 3	30	889
Reactor # 4	89	1500
Reactor # 5	49	1500
Reactor # 6	30	1500

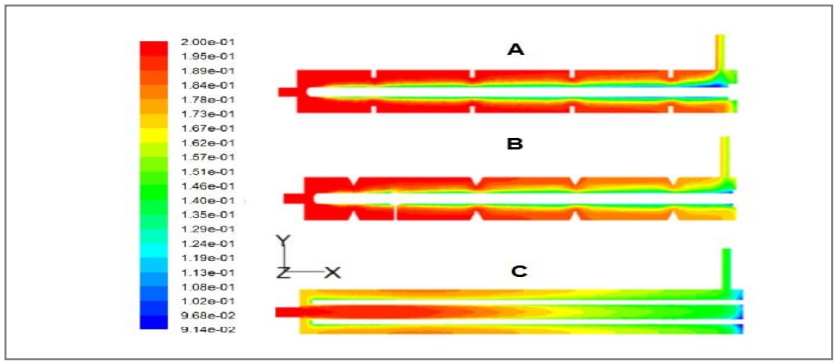

Figure14: The mass fraction of live microorganism (mass flow rate=0.45 kg/s)
A) Reactor # 1, B) Reactor # 2, C) Reactor # 3

Table 6: Performance of UV reactor for different geometries

Reactor type	Inactivation rate	Reactorvolume(m^3)	Residence time (s)	Inactivation rate per volume of reactor(m^{-3})
Main reactor	0.078	0.00571	9.39	13.66
Reactor #1	0.134	0.00571	9.39	23.46
Reactor #2	0.078	0.00187	3.07	41.71
Reactor #3	0.135	0.00042	0.69	321.42
Reactor #4	0.145	0.00910	14.97	15.93
Reactor # 5	1.015	0.00280	29.96	362.5
Reactor # 6	1.220	0.000662	7.080	1842

In order to design an efficient reactor that disinfects fluids with high UV absorption coefficients, it is important to take the following steps. First, estimate the range of UV influence using the simulation of fluence rate. Then, identify the radius of the reactor or the thickness of the moving film on the lamp. Finally, define the residence time, inlet mass flow rate and length of reactor based on the reactor radius.

5. Conclusion

This article summarizes UV reactor simulations as conducted with CFD tools. Hydrodynamic, radiation and kinetic models were developed. Solving the equations of continuity, momentum and Realizable k-ε turbulence model determined flows and velocity profiles. The fluence rate was obtained by solving the DO radiation model.

The velocity profile, fluence rate and Chick Watson kinetic models were substituted in species mass conservation

equations to calculate the live microorganism concentration profile and inactivation rate. The first simulation was done with water using available experimental data, and used to validate the reactor performance model. Subsequent simulation results indicated agreement with experimental data. Then, the applesauce simulation was conducted in accord with a power law non-Newtonian fluid model. In order to design the applesauce UV disinfection reactor, the UV penetration depth was obtained from the CFD simulations. UV absorption coefficient of applesauce is higher than water so the inactivation of microorganisms in applesauce is less than the water. Test results demonstrate that for high UV absorption fluids such as applesauce, thin film or small radius UV reactors are most

effective. Finally, appropriate reactor designs to account for the UV penetration of applesauce were proposed.

Nomenclature

C Concentration of microorganisms[mol/l]
C_0 Initialconcentration of microorganisms [mol/l]
C_μ Empirical coefficient, mixing length model (dimensionless)
D Diffusion coefficient (m^2/s)
g Gravity acceleration (m^2/s)
J Diffusion flux ($mol/m^2.s$)
k Inactivation rate constant (m^2/J)
k_s Scattering coefficient (m^{-1})
K consistency coefficient ($Pa.s^n$)
L_2 Lamp arc length (m)
L_i Distance from lamp point to current point (MPSS) (cm)
M length unit (m)
P Pressure (Pa)
r Radial distance from lamp (cm)
r_L Radius of lamp sleeve (cm)
R Reaction rate
S Path length (m)
s Scattering direction vector (m)
t Time (s)
T_r Transmissivity of the fluid (m-1)
u Velocity (m/s)
W Watt (Power unit)
z Axial distance on lamp (cm)

Greek letters
δ_{ij} Kronecker delta (Which is 1 if i and j are equal and 0 otherwise).
ρ Density (kg/m3)
σ Stefan–Boltzmann constant ($5.672\times10^{-8}Wm^{-2}K^{-4}$)
σ_w Absorption coefficient (m^{-1})
τ Stress tensor
Ω’ Solid angle about the scattering direction vector (sr)
Ω Solid angle about the propagation direction (sr)
φ Phase function for the in-scattering of photons (dimensionless)
ν Kinematic viscosity
ϕ Lamp power (W)

References:

1- Unluturk, S. K., Arastoopour, H. andKoutchma, T. (2004). "Modeling of UV dose distribution in a thin-film UV reactor for processing of apple cider."*J. Food Eng*., Vol. 65, pp. 125–136.

2- Adhikari, C., Koutchma, T. and Beecham-Bowden, T. (2005). "Evaluation of HHEVC (4, 40, 400-tris-di-B-hydroxyethyl amino triphenylacetonitrile) dye as a chemical actinometer in model buffers for UV treatment of apple juice and cider."*LWT-Food Sci. Technol*., Vol.38, No. 7, pp. 717-725.

3- Koutchma, T. and Parisi, B. (2004). "Biodosimetry of escherichia coli UV inactivation in model juices with regard to dose distribution in annular UV reactors."*J. Food Sci*., Vol. 69, No. 1, FEP14-FEP22.

4- Koutchma, T., Parisi, B. andUnluturk, S.K. (2006). "Evaluation of UV dose in flow-through reactors for fresh apple juice and cider."*Chem. Eng. Commun*., Vol. 193, pp. 715–728.

5- Keyser, M., Műller, I.A., Cilliers, F.P., Nel, W. andGouws, P.A. (2008). “Ultraviolet radiation as a non-thermal treatment for the inactivation of microorganisms in fruit juice."*Innovative Food Sci. Emerging Technol*., Vol. 9, pp. 348–354.

6- Koutchma, T., Parisi, B. andPatazca, E. (2007). "Validation of UV coiled tube reactor for fresh fruit juices."*J. Environ. Eng*., Vol. 6, pp. 319–328.

7- Oteiza, J.M., Giannuzzi, L. and Zaritzky, N. (2010). "Ultraviolet treatment of orange juice to inactivate E. coli O157:H7 as Affected by Native Microflora." *Food Bioprocess Technol.*, Vol.3, No. 4, pp. 603-614.

8- Unluturk, S., Atılgan, M.R., Handan Baysal, A. and Tarı, C. (2008). “Use of UV-C radiation as a non-thermal process for liquid egg products (LEP)."*J. Food Eng.,* Vol. 85, pp. 561-568.

9- Ducoste, J.J., Liu, D. and Linden, K. (2005). "Alternative approaches to modeling fluence distribution and microbial inactivation in Ultraviolet Reactors: Lagrangian versus Eulerian."*Environ. Eng*., Vol.131, No. 10, pp.1393–1403.

10- Duran, J.E., Taghipour, F. andMohseni, M. (2009). "CFD modeling of mass transfer in annular reactors."*Int. J. Heat Mass Transfer*, Vol. 52, pp. 5390-5401.

11- Elyasi, S. andTaghipour, F. (2006). "Simulation of UV photoreactor for water disinfection in Eulerian framework."*Chem. Eng. Sci*., Vol. 61, pp. 4741– 4749.

12- Wols, B.A., Shao, L., Uijttewaal, W.S.J., Hofman, J.A.M.H., Rietveld, L.C. andVan Dijk, J.C. (2010). "Evaluation of experimental techniques to validate numerical computations of the hydraulics inside a UV bench-scale reactor."*Chem. Eng. Sci*., Vol. 65, pp. 4491-4502.

13- Liu, D., Wu, C., Linden, K. andDucoste, J. (2007). "Numerical simulation of UV disinfection reactors: Evaluation of alternative turbulence models." *Appl. Math. Model*., Vol. 31, pp. 1753-1769.

14-Sozzi, D. andTaghipour, F. (2006). "UV reactor performance modeling by Eulerian and Lagrangianmethods."*Environ. Sci. Technol*., Vol. 40, No. 5, pp. 1609-1615.

15- Chiu, K., Lyn, D.A., Savoye, P. and Blatchley, E.R. (1999). 'Integrated UV disinfection model based on particle tracking."*Environ. Eng*., Vol. 125, No. 1, pp. 7-16.

16- Duran, J.E., Taghipour, F. and Mohseni, M. (2010). "Irradiance modeling in annular photoreactors using the finite-volume method."*J. Photochem. Photobiol. A: Chemistry*., Vol. 215, pp. 81-91.

17- Stamnes, K., Tsay, S.C., Wiscombe, W. andJayaweera, K. (1988). "Numerically stable algorithm for discrete-ordinate-method radiative transfer in multiple scattering and emitting layered media." *Appl. Optics*, 27(12), pp. 2502-2509.

18- Liou, B.T. and Wu, C.Y. (1996). "Radiative transfer in a multi-layer medium with Fresnel interfaces."*Heat Mass Transfer*, Vol. 32, No. (1-2), pp. 103-107.

19- Patankar, S.V. (1980). Numerical Heat Transfer and Fluid Flow, *Taylor and Francis*.

20- Versteeg, H. andMalalasekra, W. (2007). An Introduction to Computational Fluid Dynamics: The Finite Volume Method, 2nd Edition, *Pearson Prentice Hall*.

21- Steff, J.F. (1996). Rheological Methods in Food Process Engineering, 2nd ed., *Freeman Press*, *East Lansing, USA.*

22- Sozzi, A. andTaghipour, F. (2006). "Computational and experimental study of annular photo-reactor hydrodynamics."*Int. J. Heat Fluid Flow,* Vol. 27, pp. 1043–1053.

23- Liu, D., Ducoste, J. and Linden, K. (2004). "Evaluation of alternative fluence rate distribution models."*J. Water Supply, Res. Technol*., Vol. 56, pp. 391-408.

24- Bird, R.B., Armstrong, R.C. and Hassager, O. (1987). Dynamics of polymeric liquids: Vol. 1 *Fluid Mechanics*., 2nd ed., Wiley, New York.